Quim. Nova, Vol. 42, No. 3, 319-328, 2019 http://dx.doi.org/10.21577/0100-4042.20170322

IRON OXIDE AND Fe_2O_3/Al_2O_3 USED TO CATALYZE REMOVING HYDROGEN FROM TAIL CHLORINE AT LOW TEMPERATURE

Xi Liu[a], Ling Xue[a], Xiaoquan Chen[a], Jisheng Liu[a], Hanhan Wang[a], Jianwei Xue*[,a,], Fuxiang Li[a] and Zhiping Lv[a]
[a]College of Chemistry and Chemical Engineering, Taiyuan University of Technology, Taiyuan 030024, China

Recebido em 29/07/2018; aceito em 14/01/2019; publicado na web em 27/02/2019

The transition metal oxide, such as iron oxide and Fe_2O_3/Al_2O_3 is cheap and industrialized that are widely used to catalyze the reaction of chlorine and oxygen with hydrogen in mixture gas to remove hydrogen from tail chlorine at low temperature. The reaction gas was prepared by the same composition with industrial tail chlorine, namely Cl_2 (65% ~ 80%), O_2 (8% ~ 10%), N_2 (6% ~16%) and H_2 (1.5% ~ 4%). In this experiment, the fixed bed reactor and iron oxide or Fe_2O_3/Al_2O_3 were used as the reaction device and catalysts, respectively. The optimum conversion rate of hydrogen was 84.11% when the reaction temperature was at 70 °C with 3%wt. Fe_2O_3/Al_2O_3 and the calcination temperature was 500 °C. The results showed that the catalytic performance of Fe_2O_3/Al_2O_3 is superior to Fe_2O_3. The selectivity of the reaction of hydrogen and chloride was higher than that of hydrogen and oxygen. We also characterized the catalysts with XRD, XPS, SEM and N_2 adsorption-desorption and the results showed that the iron oxide was dispersive uniformly on the support surface.

Keywords: Fe_2O_3/Al_2O_3; remove hydrogen; tail chlorine.

INTRODUCTION

Chlor-alkali industry, developed by leaps and bounds in recent years, is a pillar industry in the field of inorganic chemical industry. The scale of its production and industrial devices has reached a new height and the world production capacity has reached more than 94 million ton. The consequent treatment of chlorine-containing tail gas should be an important problem in the production of chlor-alkali industry all over the world. The tail chlorine is a byproduct of chlorine liquefaction in the chlor-alkali industry and it is made up of chlorine (65% ~ 80%), nitrogen (6% ~ 16%), oxygen (8% ~ 10%) and hydrogen (1.5% ~ 4%)[1]. Due to the uncontrollable of hydrogen explosion, it is hard to produce the subsequent product of the tail chlorine. The presence of hydrogen was the biggest safety hazard in the treatment of tail chlorine.[2-4] Therefore, the study of how to safely and effectively remove the hydrogen in chlorine gas had attracted the attention of researchers.

The treatment process of tail chlorine was mainly composed of basicity liquid absorption,[5] synthesis of hydrochloric acid,[6] absorption – desorption, pressure swing adsorption[7] and so on. The traditional treatment of tail chlorine was usually converting hydrogen and chlorine to the hydrochloric acid by the means of combustion in chlorine-alkali industry. But in this way, chlorine in the tail chlorine was not widely used that the mainly product is hydrogen chloride. With the proposal of energy conservation, emission reduction and green development, traditional technology cannot satisfy the development of industry. Under the catalytic action of the catalyst, the hydrogen in the tail chlorine can be reduced to the utmost extent and even can be removed completely. For the reason that the problem of safety has been solved, the pure chlorine gas can be liquefied and the economic benefit has been improved.

The activated carbon was used to catalyze H_2 and Cl_2 to produce HCl in early catalytic removing hydrogen research. In 1957, Kulcsar, Geza J et al synthesized HCl by using activated carbon to catalyze Cl_2 and H_2 reaction at 250 °C.[8]

In 1962, Tanno catalyzed the gas mixture with H_2 and Cl_2 with a ceramic tube (150 ml, Φ 25 * 700 mm) at 100 ~ 400 °C, that he found the lower the gas velocity, the higher the temperature which means a higher hydrogen conversion rate. His research results ranged from 22% to 96% under different reaction condition.[9]

Further, some scholars adopted CuCl, platinum, lanthanide metals and alloys as the loaded active catalytic component to remove hydrogen from the tail-chlorine. Some research indicated that noble metals had a good catalytic performance in the reaction of Cl_2 - H_2. The catalytic system that some materials such as $LaCl_3$, KCl and $CuCl_2$ loaded on SiO_2 can catalyzed the mixture gas (95.6% Cl_2 and 2.97% H_2) to remove hydrogen at 200 ~ 400 °C and the hydrogen content can be reduced to the PPM level at 400 °C. They got the same results above when the materials changed to Pd/Al_2O_3 under the temperature of 250 ~ 260 °C.[10]

The early research of removing hydrogen reaction from the tail chlorine has developed a lot of years and the catalytic carrier was conventional activated carbon, SiO_2 and Al_2O_3. But the research still faces some problems that are waiting to be solved. The traditional reaction of removing hydrogen reaction is always the catalytic reaction of Cl_2 and H_2 that the reaction of H_2 and Cl_2 is a strong exothermic reaction.[11] The corrosion resistance of the catalytic carrier will be decreased under the high temperature and further affects the lifetime of the catalysts.

Hanhan Wang et al. studied the catalytic dehydrogenation performance of Pd/Al_2O_3 at low temperature and the following conclusions were drawn: The hydrogen conversion was 97.38% and selectivity of hydrogen-oxygen reaction was 79% when the reaction temperature was 60 °C with 1%wt. Pd/Al_2O_3. The noble metal palladium in this catalytic system needed to be reduced to carry out the catalytic reaction that is a complicated and costly process. In order to achieve industrialization, we need to find a cheap and simple catalyst to remove hydrogen from tail chlorine.[12]

This paper used iron oxide or Fe_2O_3/Al_2O_3 as catalyst to remove hydrogen from tail chlorine safely and economically.

---

*e-mail: xuejianwei@tyut.edu.cn

EXPERIMENTAL

Materials and instrumentation

All starting materials were of analytical grade and obtained from commercial sources without further purification. X-ray diffraction (XRD) of samples was performed in the range of 10-80° (2θ) with a scan speed of 8 °/min by using a Shimadzu Corporation's XRD-6000 X-ray Diffractometer with Cu Ka radiation and the Ni filter. The operating voltage was 36 kV and the tube pressure/tube current were 40 KV/30 mA. Field emission scanning electron microscopic (FE-SEM) images of samples were acquired by using a JEOL Ltd's JSM-6700F emission scanning electron microscope. X-ray photoelectron spectra (XPS) were measured on an ESCAL-ab 220iXL XPS photoelectron spectrometer produced by British VG Scientific with an Al Ka X-ray source, base vacuum 3×10^{-7} KPa, power 0.3 KW, calibration of electronic binding energy using contaminated carbon C1s internal standard. N_2 adsorption-desorption was analyzed by using a NOVA 2000 e automatic surface area and porosity analyzer produced by corporation Quanta chrome, America.

Catalyst preparation

In this experiment, cheap metal iron was selected as the active component, and the Fe_2O_3/Al_2O_3 was prepared by incipient-wetness impregnated method. In the experiment, the active component of catalyst was Fe and we selected Fe $(NO_3)_3{\cdot}9H_2O$ as the precursors of impregnation. After calculation, a series of Fe $(NO_3)_3$ solutions with a certain mass fraction were prepared. Firstly, the volume of the impregnated solution of 1 g γ-Al_2O_3 was determined by deionized water, and the volume was 1.175 mL. 1.0 g γ-Al_2O_3 powder was impregnated into 1.175 mL Fe $(NO_3)_3$ solution for 24 h at room temperature so that the Fe^{3+} can uniformly dispersed on the surface of γ-Al_2O_3. Then the sample was dried in a drying oven for 12 h and we got Fe $(NO_3)_3/Al_2O_3$. Finally, the dried sample was calcined in muffle furnace at air atmosphere for 4 h and the final product was Fe_2O_3/Al_2O_3.[13,14] The achieved samples were collected into the sample bag and marked with labels.

The loading amounts of the catalysts were 0.5%, 0.8%, 1%, 2%, 3%, 4%, 5%, 8%, 10% and the mass concentrations of the impregnated solution were 0.031 g mL^{-1}, 0.049 g mL^{-1}, 0.062 g mL^{-1}, 0.123 g mL^{-1}, 0.185 g mL^{-1}, 0.246 g mL^{-1}, 0.308 g mL^{-1}, 0.493 g mL^{-1}, 0.616 g mL^{-1}, respectively.

Catalytic removing hydrogen reaction of tail chlorine

As is presented in Figure 1, the as-prepared samples were put into a fixed-bed reactor system to evaluate its catalytic performance. The procedure of tail chlorine separation experiments was carried out as follows. Firstly, we placed 0.5 g catalyst into the fixed-bed reactor. Then, the gas line of the reaction device was purged with nitrogen at room temperature for 10 minutes and the air in the gas line was removed completely. At last, the simulated mixture gas was brought into the reactor at a specific reaction temperature. In order to acquire the according experimental conditions, the simulated mixture gas was composed of Cl_2, O_2, H_2 and N_2 according to the composition of industrial tail chlorine. The content of H_2, O_2 and N_2 that remaining in the mixture gas after the catalytic removing hydrogen reaction were analyzed periodically by GC (Gas Chromatograph). The conversion rate and the selectivity of hydrogen were calculated by comparing the content of each component before and after the reaction.

RESULTS AND DISCUSSION

The tail chlorine removing hydrogen performance of iron oxide catalyst

The influence of reaction temperature on catalytic removing hydrogen of iron oxide catalyst was analyzed as follows. As shown in Figure 2, the initial conversion rate of hydrogen could surpass 90% when the reaction temperature was above 50 °C with Fe_2O_3 as catalyst. But, the total conversion rate of hydrogen decreased with the time increased. At first, the downward trend was relatively slow, and when the reaction was near the end, the conversion rate of hydrogen decreased rapidly. It is indicated that the stability of iron oxide to catalyze removing hydrogen from tail chlorine was low. This is because iron oxide has good adsorption property in the process of reaction gas go across the catalyst and it can adsorb the reaction gas very quickly, making the gas react on the surface of catalyst. However, the surface area of iron oxide powder was small, leading to the declination of the reaction performance.

What's more, the total conversion rate of hydrogen is increased with the enhancement of the reaction temperature, which was especially obvious at more than 100 °C. For the reason that the elevated temperature can accelerate the reaction rate, making the reaction velocity of hydrogen and oxygen or chloride increase that further make the total conversion rate of hydrogen increase. At the same time, the rate of adsorption and desorption of the gas on the surface of catalyst would be accelerated which can provide more reaction surface for unreacted gas.

As shown in Figure 2 and Figure 3, with the temperature increased, the conversion rate of hydrogen is continuously rising, indicating that the increase of temperature can promote the catalytic reaction. Further observation, the conversion rate in the rising part

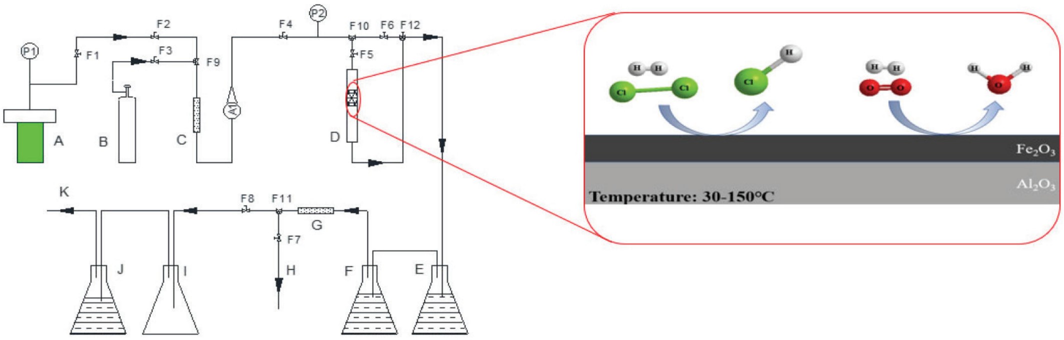

Figure 1. *The device for removing hydrogen from the tail chlorine. (A) gas tank, (B) Nitrogen cylinder, (C) calcium chloride desiccator, (D) fixed-bed reactor, (E,F) sodium hydroxide solution, (G) Calcium oxide drier, (H) sampling device, (I) surge flask, (J) sodium carbonate solution, (K) Reaction exhaust outlet. F1-F8, Needle valves; F9-F11, Three Direct Links; F12, Spherical three-way valve; P1, P2, vacuum gauges; A1, rotor flowmeter*

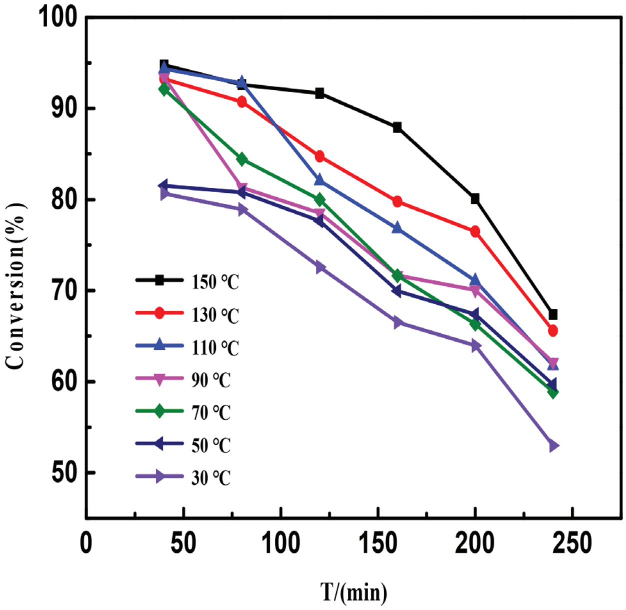

Figure 2. *Total conversion rate of hydrogen in the catalytic reaction of* Fe_2O_3 *at different reaction temperature*

can be divided into three stages. When the temperature ranged from 30 °C to 70 °C, the rising trend was fast and the conversion rate of hydrogen was 75.56% at 70 °C. The rising trend was changed gentle between 70 °C and 90 °C. The conversion rate of hydrogen began to increase in the region of 90 °C to 150 °C, but its amplitude was inferior to the first paragraph. After analyzing the results of Figure 2 and Figure 3 and combining the consideration of the problem of industrial economic efficiency, we believe that 70 °C is the optimum reaction temperature of iron oxide to catalyze removing hydrogen from tail chlorine.

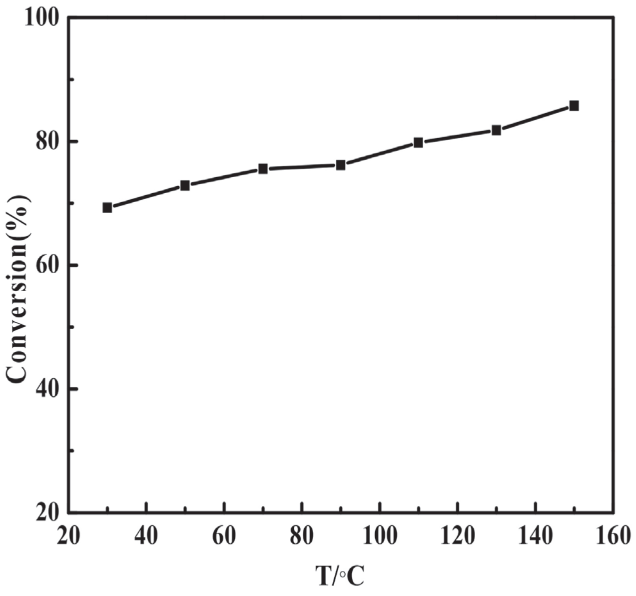

Figure 3. *Average conversion rate of hydrogen in the catalytic reaction of* Fe_2O_3 *at different reaction temperature*

As shown in Figure 4, the selectivity of hydrogen and chloride reaction firstly rose and then fell with the maximum of 69.33% under the temperature of 90 °C and the selectivity of hydrogen and oxygen reaction decreased firstly and then increased. The selectivity of hydrogen and chloride reaction were generally higher than that of hydrogen and oxygen reaction during the entire reaction temperature range, so iron oxide had a better catalytic activity in the reaction of hydrogen and chloride.

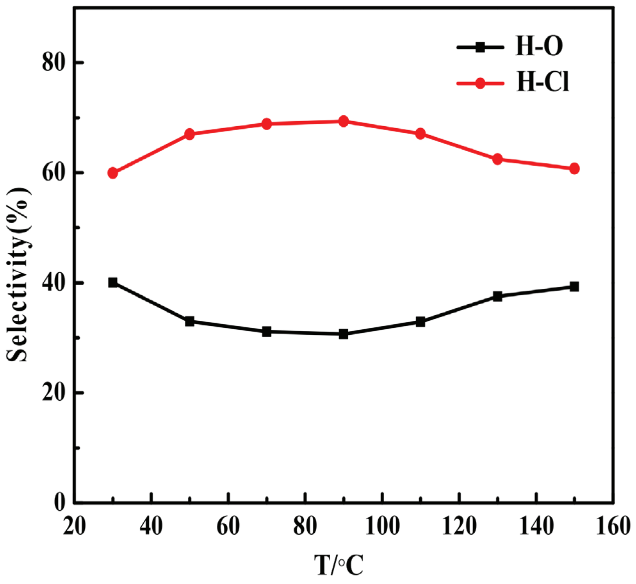

Figure 4. *Average selectivity of hydrogen in the catalytic reaction of* Fe_2O_3 *at different reaction temperature*

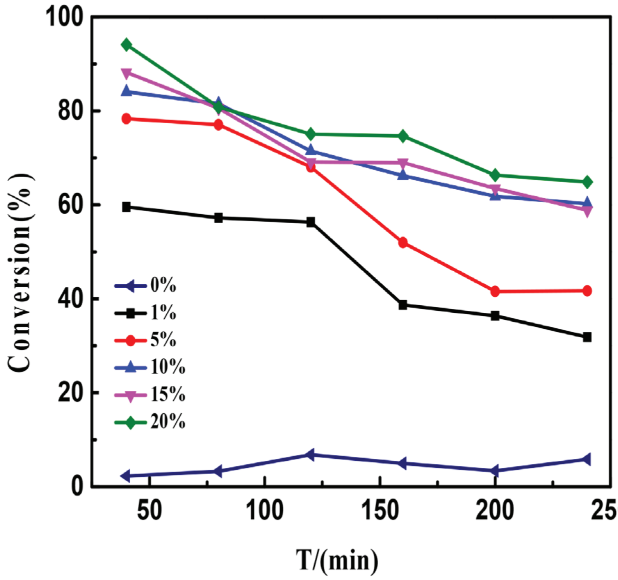

Figure 5. *Total conversion rate of hydrogen in the catalytic reaction of ferric oxide and alumina by mechanical mixing at 70 °C*

The analysis of removing hydrogen performance by the means of mechanically mixing the iron oxide with aluminum oxide is as follows. The percentage content in Figure 5 is the effective content of iron oxide. The purpose of adding alumina was to increase the surface area of the iron oxide, making up the deficiency of the pure iron oxide as a catalyst which cannot provide better surface. It can be seen from the diagram, the total conversion rate of hydrogen was increased with the content of iron oxide increased. The total conversion rate of hydrogen was 94% when the content of iron oxide was 20%. It can be illustrated that the iron oxide was the active center with the main catalytic effect in this catalytic system. The results above provide a powerful support for the further discussion about the iron oxide coated on alumina.

The performance of Fe_2O_3/Al_2O_3 remove hydrogen from tail chlorine

The influence of reaction temperature on catalytic removing hydrogen of Fe_2O_3/Al_2O_3 was analyzed as follows. This test is to explore the effect of reaction temperature on the catalytic activity of a loaded iron oxide catalyst. In the following experiments, the content of iron oxide was 1% and the calcination temperature was 550 °C.

As shown in Figure 6, the total conversion rate of hydrogen decreased rapidly at first and then declined gradually under the same reaction temperature. The phenomenon can be concluded of that the loaded catalyst has better stability than the un-loaded catalyst. When the iron oxide loaded on the alumina which used as catalytic carrier can provide a larger surface area and a stable structure for catalytic action that can keep a good stability in a certain time. At the meantime, the catalytic activity of catalysts and the total conversion rate of hydrogen increased with the reaction temperature elevated. As a result, the conversion rate of the reaction increased due to the change of the reaction temperature. For the velocity of gas transfer increased under the higher temperature, leading to the enhancement of the adsorption and desorption rate of the mixture gas on the surface of alumina.

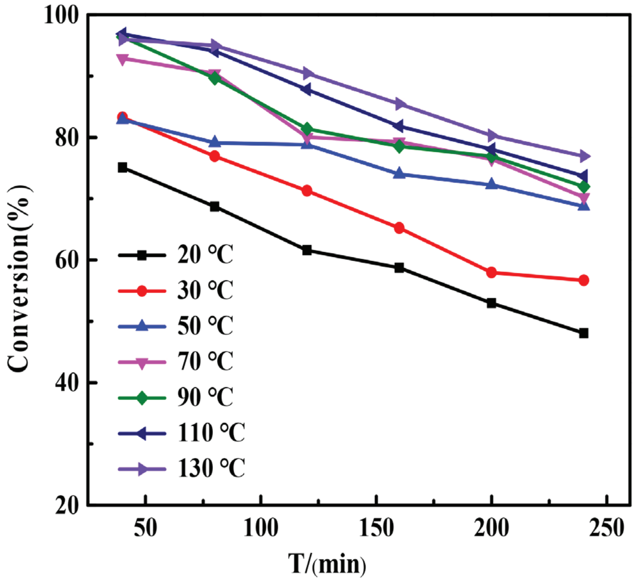

Figure 6. *Total conversion rate of hydrogen in the catalytic reaction of* Fe_2O_3/Al_2O_3 *at different reaction temperature*

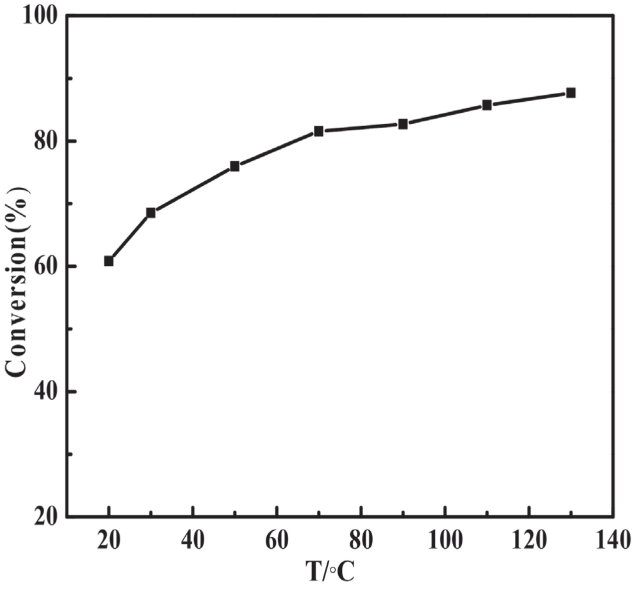

Figure 7. *Average conversion rate of hydrogen in the catalytic reaction of* Fe_2O_3/Al_2O_3 *at different reaction temperature*

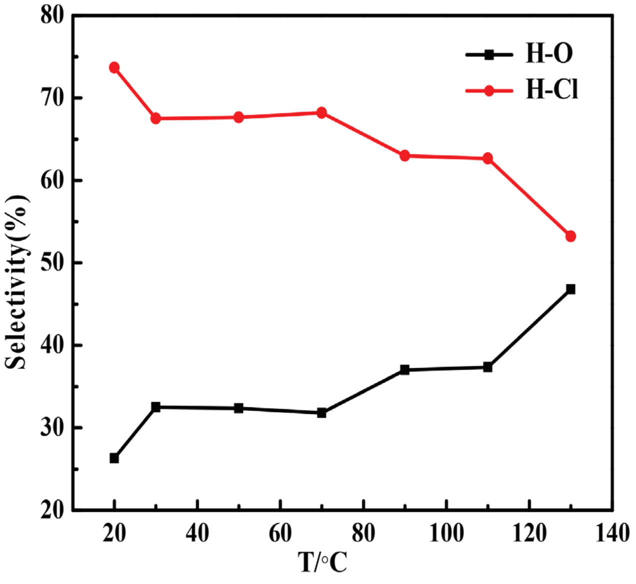

Figure 8. *Average selectivity of hydrogen in the catalytic reaction of* Fe_2O_3/Al_2O_3 *at different reaction temperature*

As shown in Figure 7, the conversion rate of hydrogen was continuously rising with the increase of reaction temperature. The rising trend of the conversion rate of hydrogen is steep with the temperature is low. And the condition is a little different in the high temperature region that the rising trend of the conversion rate of hydrogen is getting gentle. When the temperature ranged from 20 °C to 70 °C, the fluidity of mixture gas changed more and more fast which further improved the reaction speed with a conversion rate of hydrogen was 81.54% at 70 °C. When the temperature ranged from 70 °C to 130 °C, we can see the rising trend of the conversion rate of hydrogen was gentle due to the limited active sites.

Figure 8 shows the selectivity of the hydrogen-chlorine and hydrogen-oxygen reaction. The selectivity of the hydrogen-chlorine reaction and the hydrogen-oxygen reaction was decreased and increased respectively in the region of 20 °C to 130 °C. We can draw a conclusion that the hydrogen-oxygen reaction prefers a high temperature and the hydrogen-chlorine reaction prefers a low temperature. The selectivity of hydrogen and chloride reaction were generally higher than that of hydrogen and oxygen reaction during the full reaction temperature range. Considering the performance of loaded iron oxide catalyst and unloaded iron oxide catalyst in the catalytic removing hydrogen, the hydrogen and chloride reaction took precedence over the hydrogen and oxygen reaction.

The analysis of the influence of calcination temperature on catalytic removing hydrogen of Fe_2O_3/Al_2O_3 was as follows. The calcination temperature will have an effect on the internal structure of catalyst such as the crystal shape of catalyst which would affect the catalytic effect. Therefore, it was necessary to explore the influence of different calcination temperature on the catalytic effect of Fe_2O_3/Al_2O_3 catalyst. We had explored the performance of the catalysts under different calcination temperature of 300 °C, 400 °C, 450 °C, 500 °C, 550 °C and 600 °C with the reaction temperature of 70 °C and the catalysts loading amount was 1%.

As shown in Figure 9, all of the curves perform the same trend that the total conversion rate of hydrogen was decreased with the time went on. This was because that the reaction will generate water and hydrogen chloride and the product cannot be separated in time, which would cause the catalyst to combine with water or react with acid. And the reduction of active sites of catalyst lead to the decrease of catalytic activity and the conversion rate of hydrogen. It can be seen that the activity of the catalytic performance was different at different calcination temperature. When the calcination temperature was 500 °C, the catalyst performed the optimum catalytic activity of all the reaction temperature.

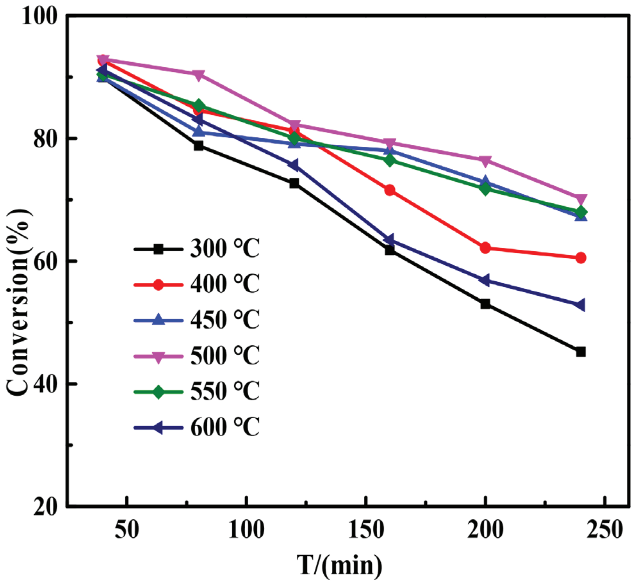

Figure 9. *Total conversion rate of hydrogen in the catalytic reaction of* Fe_2O_3*/*Al_2O_3 *at different calcination temperature*

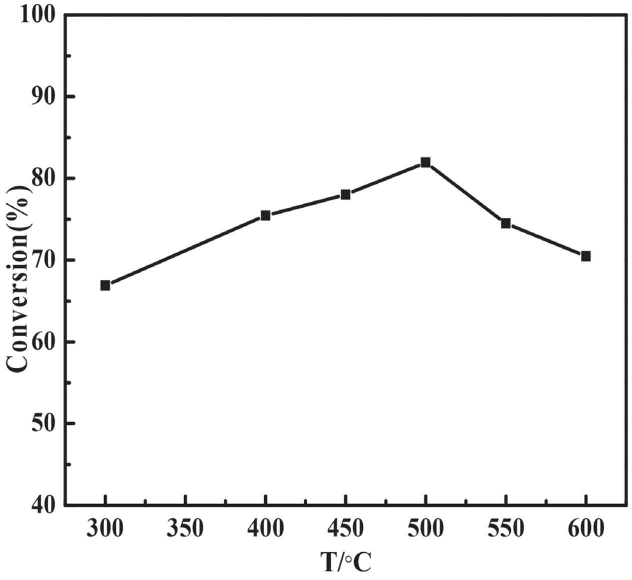

Figure 10. *Average conversion rate of hydrogen in the catalytic reaction of* Fe_2O_3*/*Al_2O_3 *at different calcination temperature*

It can be more directly analyzed from Figure 10 that the influence of calcination temperature on catalytic activity was increased at first and then decreased. The average conversion rate of hydrogen can reach to 81.92% under the calcination temperature of 500 °C. Lower calcination temperature leads to the unstable structure of catalyst that the iron oxide is easy to fall off from alumina during the catalytic reaction. With the increase of the calcination temperature, the catalyst is relatively stable. But the catalytic active of the catalyst will reduce when the calcination temperature surpasses 500 °C for the reason that the carrier will shrink under the high temperature which lead to the collapse of the holes in the catalyst. So, the specific surface area of the catalyst will decrease and further affect the catalytic performance of the catalyst.[15]

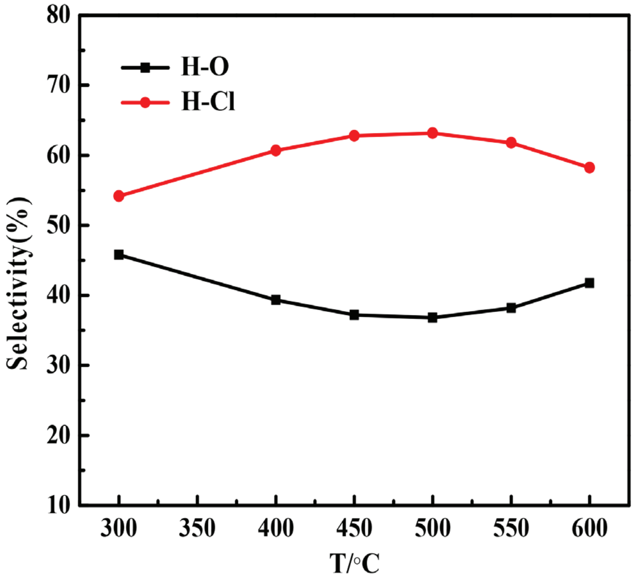

Figure 11. *Selectivity of hydrogen in the catalytic reaction of* Fe_2O_3*/*Al_2O_3 *at different calcination temperature*

The selectivity of hydrogen and chloride reaction and hydrogen and oxygen reaction is shown in Figure 11. With the enhancement of the temperature, the selectivity of hydrogen and chloride reaction was increased from 300 °C to 500 °C and decreased from 500 °C to 600 °C with the peak value of the selectivity has reached to 63.18% under the calcination temperature of 500 °C. Otherwise, the selectivity of hydrogen and oxygen reaction had a different performance with a downtrend from 300 °C to 500 °C and an uptrend from 500 °C to 600 °C. It can be seen from Figure 11, the selectivity of hydrogen and chloride reaction was greater than that of hydrogen and oxygen reaction within a certain range of calcination temperature. According to the analysis above, 500 °C is the best calcination temperature of the catalytic reaction and the oxide catalyst is more beneficial to the reaction of hydrogen and chlorine to generate hydrogen chloride.

The loading amount of Fe_2O_3 in the reaction of Fe_2O_3/Al_2O_3 catalytic removing hydrogen is analyzed as follows. The suitable loading capacity of Fe_2O_3 will have a good effect on the catalytic reaction. So, we explored different Fe_2O_3 loading ratios of 0.5%, 0.8%, 1%, 2%, 3%, 4%, 5%, 8% and 10% in Fe_2O_3/Al_2O_3 catalyst. The reaction temperature and the calcination temperature of catalyst are 70 °C and 500 °C, respectively.

The change trend in Figure 12 can be divided into four stages. Firstly, the conversion rate of hydrogen soared rapidly with the loading amount from 0.8% to 1.0%. Then, the rising trend has slowed down with the loading amount from 1.0% to 2.0%. And the average conversion rate of hydrogen keeps a stable state with the loading amount from 3.0% to 5.0%. At last, the average conversion rate of hydrogen has a slowly downtrend with the loading amount from 5.0% to 8.0%. For the reason that the catalytic property of Fe_2O_3/Al_2O_3 catalyst is related to the loading amount of Fe_2O_3 which act as the active component in this catalytic system. So, the catalytic activity performs poor when the ratio amount of Fe_2O_3 is few and the conversion rate of hydrogen is good when the loading amount is large. However, the excess loading amount of Fe_2O_3 will not bring a good result. On the contrary, loading the excess Fe_2O_3 will block the pores and holes of the catalytic carrier and further reduce the catalytic reactive sites. As a result, the catalytic activity and the total conversion rate of hydrogen are decreased. According to the experimental data, iron oxide particles could be uniformly dispersed on the surface of the catalytic carrier and the catalytic activity is the best when the loading amount is 3% wt.

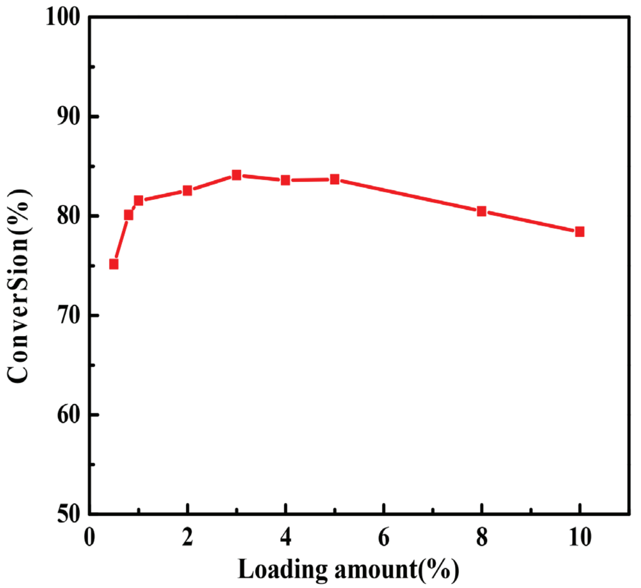

Figure 12. *Average conversion rate of hydrogen in the catalytic reaction of Fe_2O_3/Al_2O_3 with different loading amount*

Table 1 reflects the experiment data of the total conversion rate of hydrogen with different reaction time and different loading amount. It can be seen from Table 1 that the catalytic removing hydrogen activity of catalyst decreased monotonously at each loading amount. The catalytic stability of all the samples is of little difference at first. As the reaction time goes by, the catalytic stability of the low loading amount samples exhibits poor catalytic performance and the catalytic stability of the high loading amount samples exhibit good catalytic performance.

Table 1. Conversion rate of hydrogen in the catalytic reaction of Fe_2O_3/Al_2O_3 with different loading amount

Loading amount	Time					
	40 min	80 min	120 min	160 min	200 min	240 min
0.5%	90.25	85.42	74.78	71.84	68.77	59.88
0.8%	94.79	93.53	89.13	77.02	64.97	61.23
1%	92.87	90.42	80.02	79.28	76.44	70.23
2%	93.39	89.41	88.84	79.57	76.42	67.58
3%	93.94	92.15	90.38	84.31	77.49	66.42
4%	95.32	91.68	86.48	86.45	74.21	68.29
5%	93.15	85.00	84.48	83.83	78.70	76.94
8%	88.02	85.56	83.55	78.09	74.32	60.95
10%	96.84	86.88	79.60	74.47	72.81	72.18

The XRD patterns of iron oxide catalyst.

The XRD patterns of the iron oxide catalyst under different reaction temperature are exhibit in Figure 13. The characteristic diffraction peaks of α-Fe_2O_3 were obtained at 24.1°, 33.0°, 35.5°,40.6°, 49.3°, 53.9°, 62.2°, and 63.9°.[16] The peak strength of all the α-Fe_2O_3 catalysts has no significant change after catalytic reaction at different temperature. Because the dosage of reaction catalyst is big and the catalytic reaction will not change the crystal structure of α-Fe_2O_3 catalysts. So, the peak strength of all the α-Fe_2O_3 catalysts exhibit a good thermal stability.

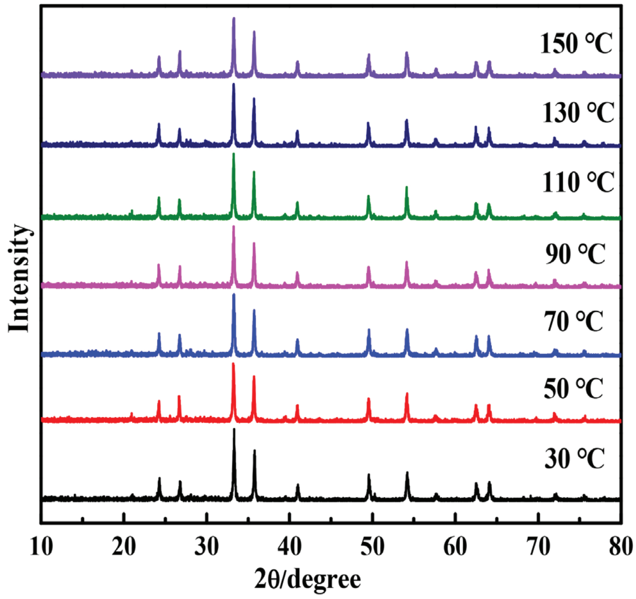

Figure 13. *XRD patterns of iron oxide catalyst indifferent reaction temperature*

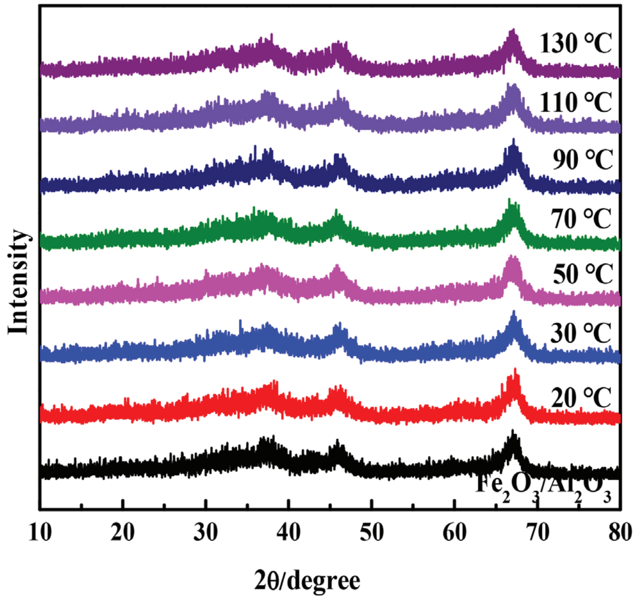

Figure 14. *XRD patterns of Fe_2O_3/Al_2O_3 catalyst at different reaction temperature*

As presented in Figure 14, all the Fe_2O_3/Al_2O_3 samples are loaded with 1%wt. Fe_2O_3 under the calcination temperature of 550 °C and the reaction temperature different. Compared with unreacted Fe_2O_3/Al_2O_3 samples, the location and strength of the characteristic diffraction peaks have no difference after catalytic reaction at different temperature. It is illustrated that the catalytic reaction at low temperature has no effect on the crystal structure of the catalysts.

As presented in Figure 15, all the Fe_2O_3/Al_2O_3 samples are loaded with 1%wt. Fe_2O_3 under the reaction temperature of 70 °C and the calcination temperature is different. The characteristic peak of α-Fe_2O_3 was not obvious when the calcination temperature is not high and the strength of peak is stronger with the calcination temperature increased. Otherwise, the strength of peak decreased with the temperature over 500 °C. The low temperature was insufficient to activate the lattice of iron oxide which lead to the inconspicuous of the characteristic peak. And the grain size of iron oxide increased with the temperature increased which reduced the surface area of the carrier and weakened the activity of catalyst. The strong diffraction peaks emerged at the calcination temperature of 500 °C which is in consistent with the optimal temperature in removing hydrogen performance of the catalysts discussed above.

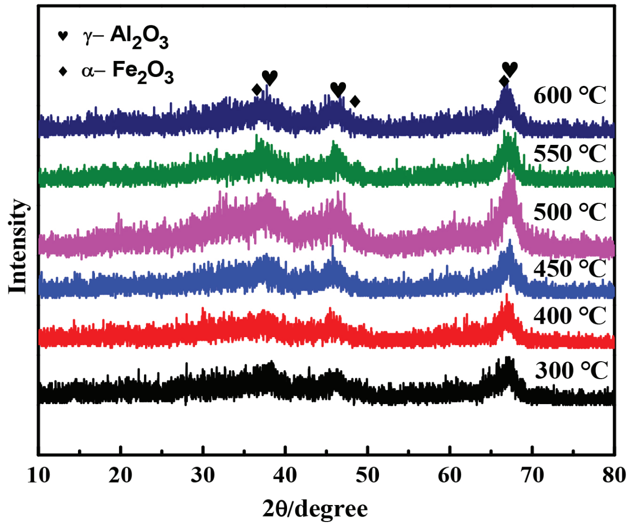

Figure 15. *XRD patterns of Fe_2O_3/Al_2O_3 catalyst at different calcination temperature*

The XRD patterns of Fe_2O_3/Al_2O_3 catalyst with different loading amount under the calcination temperature of 500 °C and the reaction temperature was 70 °C are presented in Figure 16. The diffraction peaks located at 37.1°, 45.5° and 67.1° are correspond to γ-Al_2O_3 and the peaks at 24.7°, 33.1°, 35.5°, 40.8°, 49.4°, 62.5° and 63.9° are attribute to α-Fe_2O_3 according to the reference article.[17] The strength of the diffraction peaks was strengthened with the increase of the loading amounts which proves the existence of iron in the form of α-Fe_2O_3.

The XRD patterns of Fe_2O_3/Al_2O_3 catalyst under different conditions are presented in Figure 17 and the diffraction peaks of the samples varies greatly. Although the loading amount of iron oxide by the means of mechanical mixing is relatively few in the catalyst, the diffraction peak of α-Fe_2O_3 is remain significant. However, the overall strength of the diffraction peak is still weak. The typical XRD peaks corresponding to the iron oxide are not obvious in the Fe_2O_3/Al_2O_3 samples which is ascribe to the relatively low content and the iron oxide presented a highly dispersed state on the surface of the carrier.

The SEM images of Fe_2O_3/Al_2O_3

Figure 18 shows the SEM images of Fe_2O_3/Al_2O_3 samples with different loading amounts before and after catalytic reaction. It can be seen from b, d and f, the impregnation method can effectively load iron onto the carrier alumina. Although the iron can disperse uniformly on the surface of carrier alumina with a loading amount of 1%wt., the performance of catalytic removing hydrogen is still low for the reason that the loading amount is relatively few and the shortage of active center. When the loading amount reached to 5%wt., the aggregation state appeared that would block the

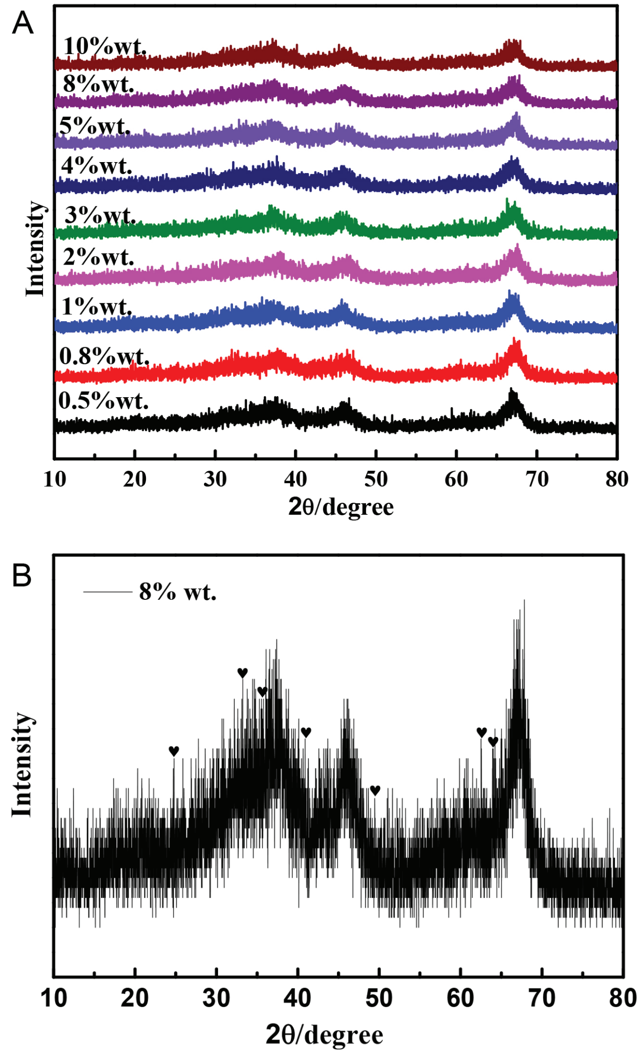

Figure 16. *XRD patterns of Fe_2O_3/Al_2O_3 catalyst at different loading*

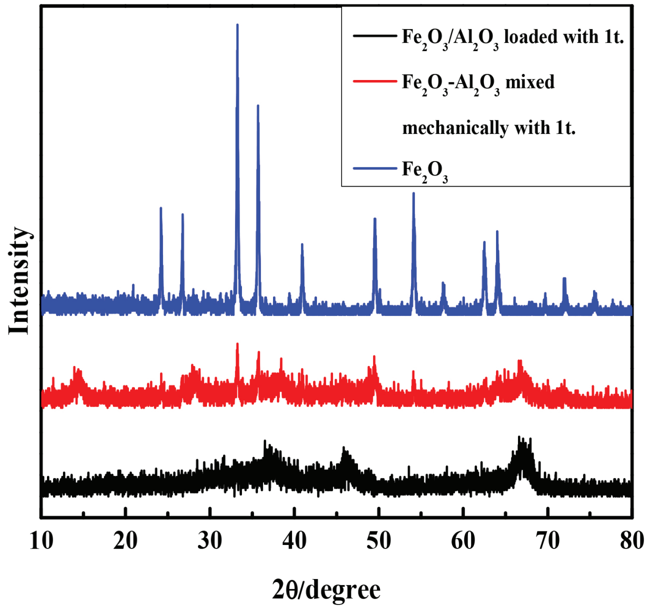

Figure 17. *XRD patterns of Fe_2O_3/Al_2O_3 catalyst at different states*

micropore structure of the carrier and reduce the catalytic activity of the catalyst. The active ingredient of catalyst is uniformly dispersed on the surface of carrier when the loading amount of the catalyst is 3%wt. It not only provides more catalytic active sites but also a certain of pore structure which is beneficial to the performance of catalytic removing hydrogen. The surface of the catalyst samples in images c (e, g) is rougher than that of the images b (d, f) and the pore size of the catalysts become large. This indicated that partial of the loaded iron oxide had reacted and it is consistent with the formation of iron chloride in the Fe_2O_3/Al_2O_3 catalyst after reaction detected in titration analysis.

The XPS spectra of 3%Fe_2O_3/Al_2O_3

As is presented in Figure 19, we can see a $Fe^0 2p_{3/2}$ peak and a $Fe^0 2p_{1/2}$ peak located at 711.4 eV and 725.1 eV respectively before

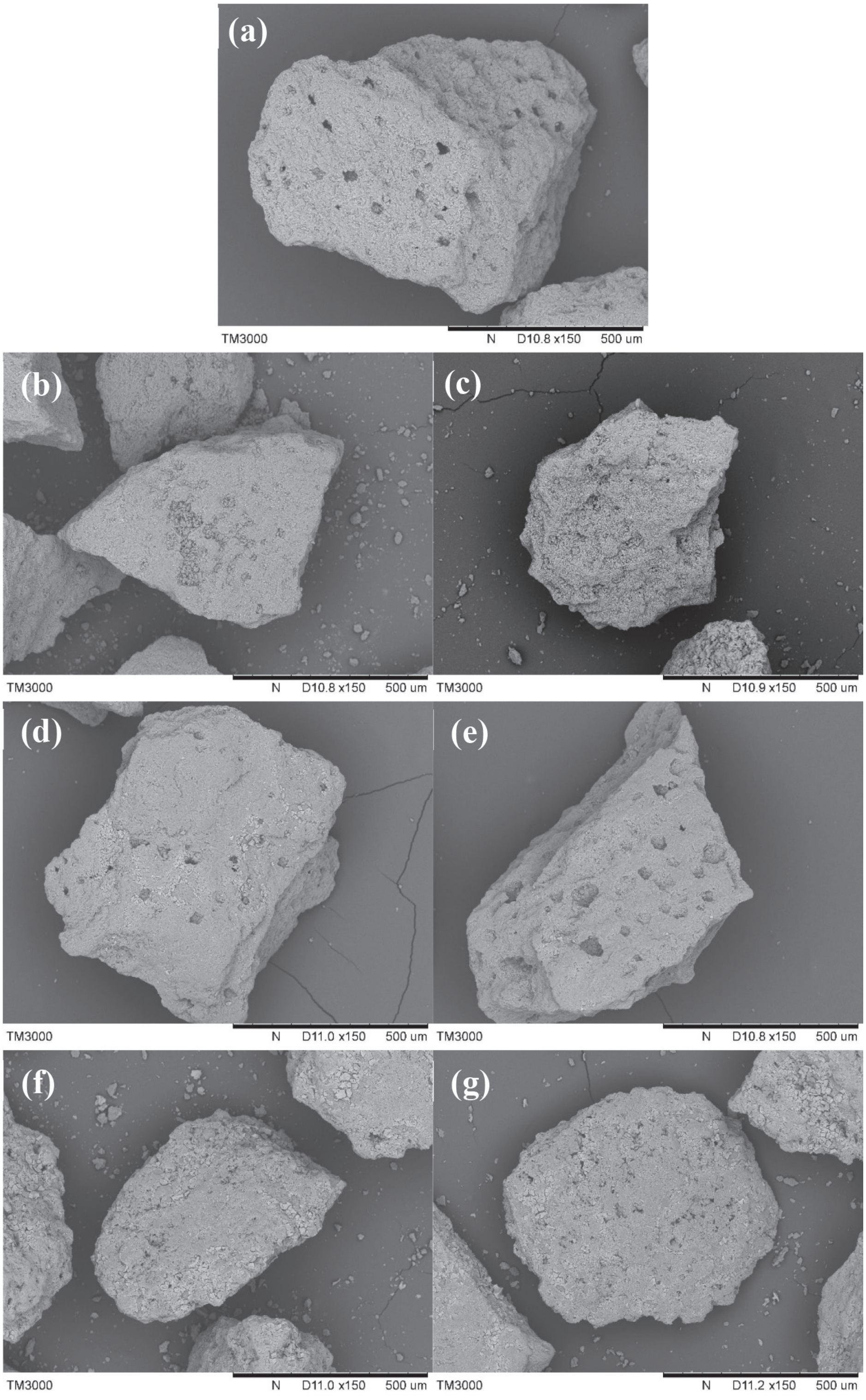

Figure 18. *SEM images of Fe_2O_3/Al_2O_3. (a)Al_2O_3; (b)1%Fe_2O_3/Al_2O_3; (c)1%Fe_2O_3/Al_2O_3 after reaction; (d)3%Fe_2O_3/Al_2O_3; (e)3%Fe_2O_3/Al_2O_3 after reaction; (f)5%Fe_2O_3/Al_2O_3; (g)5%Fe_2O_3/Al_2O_3 after reaction*

reaction. And the two peaks have a slight shift towards to a lower binding energy correspond to 710.8 eV and 724.8 eV after reaction. According to the literature,[18,19] it is the characteristic peak of Fe_2O_3 and we could confirm that the active component in Fe_2O_3/Al_2O_3 is Fe_2O_3. The shift of peak location before and after reaction is attribute to the loading of iron oxide which generated a small quantity of Fe^{3+} after the catalytic reaction. So, we can confirm that the active ingredient of the catalyst in the reaction is Fe_2O_3.

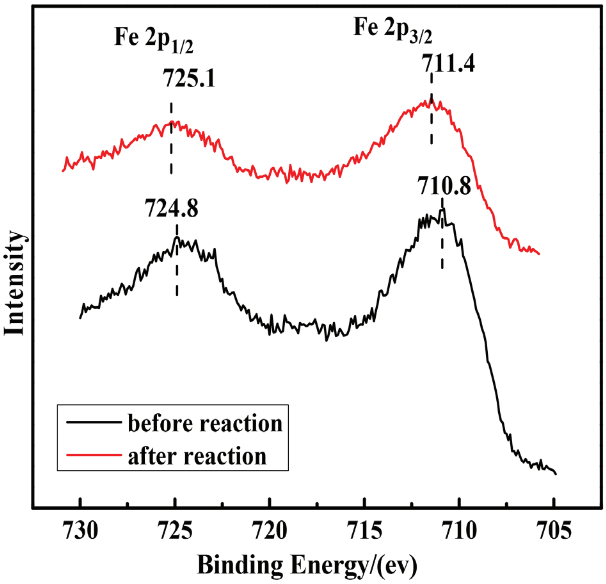

Figure 19. XPS spectra of 3%Fe_2O_3/Al_2O_3

The N_2 adsorption-desorption equilibrium curves of Fe_2O_3/Al_2O_3

As presented in Figure 20, the curves belonged to type IV isotherm[20] curve and the shape of the hysteresis loop was H3 type. From the picture, we can observe that the adsorption material in this experiment is single layer saturated adsorption and the pore diameters are not uniform. At the meantime, the material has narrow slit structure and the loading type was made up of sheet particles. We also find that the pore structure of the catalyst has not changed significantly before and after the loading and reaction from the comparison of the curves of a, b and c.

BJH model was used to analyze the pore diameter distribution. It can be seen that the pore size distribution of carrier before loading is about 7.6 nm from the analysis of Figure 21 and Table 2. Furthermore, there is a new peak at about 8 nm after loading, which is attributed to the impregnation liquid enter the internal tunnel of γ-Al_2O_3 and damage its structure in the process of impregnation. Both the pore diameter and surface area of the catalyst after reaction are all increased slightly compared with the catalyst before reaction. This phenomenon may be ascribed to the process that the catalyst is chlorinated to iron chloride during the catalytic removing hydrogen reaction. And the iron chloride sublimes and breaks away from the carrier.

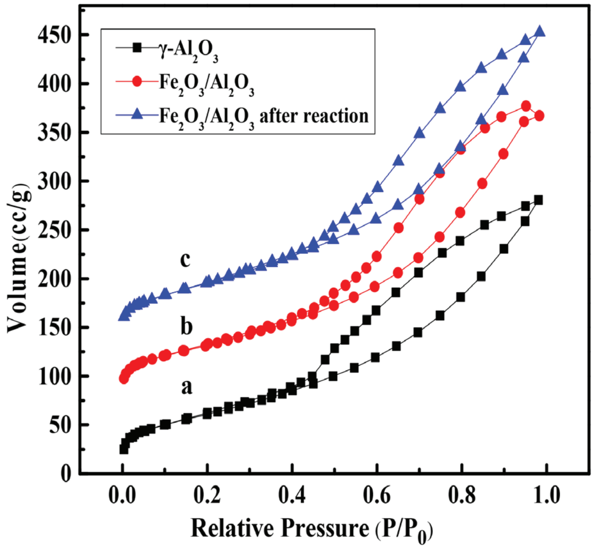

Figure 20. N_2 adsorption-desorption equilibrium curves

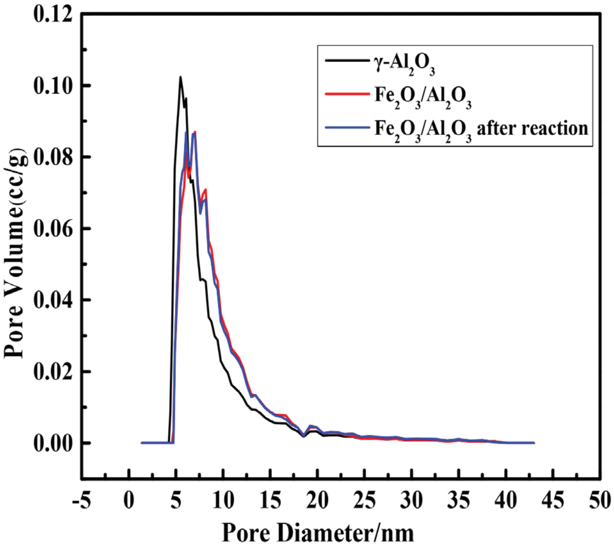

Figure 21. Pore dimension distribution

CONCLUSION

From the analysis of the iron oxide catalysts for catalytic removing hydrogen reaction performance, we can see that the conversion rate of hydrogen performs good in the catalytic reaction with iron oxide at first. However, the conversion rate of hydrogen decreased rapidly as the reaction continues due to the poor stability of iron oxide.

Compared with iron oxide catalyst, the stability of Fe_2O_3/Al_2O_3 catalyst is significantly improved. And when the reaction continues, the conversion rate of hydrogen decreased slowly. We also find the optimal reaction condition is 1%wt. Fe_2O_3 loads on Fe_2O_3/Al_2O_3 catalyst with the calcination temperature of 500 °C under the reaction temperature of 70 °C.

Table 2. Pore size and surface area distribution of γ-Al_2O_3, Fe_2O_3/Al_2O_3 and Fe_2O_3/Al_2O_3 after reaction

	Surface Area(ABET)/m^2 g^{-1}	Pore Volume/cc g^{-1}	Pore Diameter/nm
γ-Al_2O_3	229.808	0.4373	7.6178
Fe_2O_3/Al_2O_3 before reaction	229.625	0.4554	8.1136
Fe_2O_3/Al_2O_3 after reaction	237.746	0.4875	8.2028

Through the iron oxide is a kind of catalytic active component in the reaction of catalytic removing hydrogen by the analysis of the selectivity of iron oxide and Fe_2O_3/Al_2O_3, the selectivity of hydrogen and chlorine is greater than the selectivity of hydrogen and oxygen. It could be confirmed that iron oxide is more advantageous to catalyze the reaction of hydrogen and chlorine.

Both of the active components in loaded and unloaded samples of Fe_2O_3/Al_2O_3 are α-Fe_2O_3 in this study by the analysis of XRD characterization. From the XPS characterization, the active components of Fe_2O_3/Al_2O_3 are not changed before and after the catalytic reaction. It can be clearly and intuitively observed that Fe_2O_3 disperse on the surface of the carrier uniformly when the loading amount is 3%wt. by the observation of SEM. From the N_2 adsorption-desorption isotherms of the catalyst, it is clearly confirmed that the surface area and pore diameter of the carrier reduces slightly before and after loading Fe_2O_3. However, the surface area and pore diameter of the catalyst increases slightly after reaction which ascribe to the sublimation of iron chloride.

ACKNOWLEDGEMENTS

The authors thank the National Natural Science Foundation of China (No. 50972097) and the Natural Science Foundation of Shanxi (No.2008011025) for supporting this work.

REFERENCES

1. Liu, G. K.; Lin, F. J.; *Chlor-Alkali Ind.* **2006**, *3*, 30.
2. Pugh, D.; Bosauder, P.; Parnell, M.; *Appita J.* **2017**, *7*, 116.
3. Peantong, S.; Tangjitsitcharoen, S.; *5th International Conference on Manufacturing, Optimization, Industrial and Material Engineering (MOIME)*, Bali, Indonesia, 2016.
4. Kucinski, R. E.; Gerner, H. M. B.; *Mod. Chlor-Alkali Technol.* **1995**, *6*, 89.
5. Uchino, F.; Takada, K.; Kikuchi, A.; *Pat. JP 07096133* **1995**.
6. Zheng, J.; *China Chlor-Alkali* **2001**, *1*, 38.
7. Kong, X. Z.; *Cryogenics* **1999**, *4*, 328.
8. Kulcsar, G. J.; Kulcsar-Novakova, M.; *Acad. Repub. Pop. Rom., Fil. Cluj, Stud. Cercet. Chim.* **1956**, *7*, 119.
9. Tanno, H.; *Pat. JPS37-10417* **1962**. *(CAN60:P66379)*
10. Pieters, W. J. M.; Wenger, F. *US Pat. 4224293* **1980**. *(CAN93:P207001)*
11. Otto, D.; Sidney, W. B.; *J. Phys. Chem. A* **2000**, *104*, 777.
12. Wang, H. H.; Lu, T. T.; Li, Y. N.; Wu, B.; Xue, J. W.; Li, F. X.; Lv, Z. P.; *Journal of Chemistry* **2016**, ID 5620316.
13. Choi, P. H.; Jun, K. W.; Lee, S. J.; Choi, M. J.; Lee, K. W.; *Catal. Lett.* **1996**, *40*, 115.
14. Prasad, P. S. S.; Bae, J. W.; Jun, K. W.; Lee, K. W.; *Catal. Surv. Asia* **2008**, *12*, 170.
15. Hao, Q. L.; Wang, H.; Liu, F. X.; Bai, L.; Zhang, Z. X.; Xiang, H. W.; Li, Y. W.; *Chin. J. Catal.* **2005**, *26*, 340.
16. Wang, L. L.; Wu, B. S.; Li, Y. W.; *Chin. J. Catal.* **2011**, *32*, 495.
17. Liu, T.; Yu, Z. L.; Li, G.; Guo, S.; Shan, J.; Li, C. Y.; Fang, Y. T.; *Int. J. Hydrogen Energy* **2018**, *43*, 19384.
18. Bukhtiyarova, G. A.; Bukhtiyarov, V. I.; Sakaeva, N. S.; Kaichev, V. V.; Zolotovskii, B. P.; *J. Mol. Catal. A: Chem.* **2000**, *58*, 251.
19. Yamashita, T.; Hayes, P.; *Appl. Surf. Sci.* **2008**, *254*, 2441.
20. Gregg, S. J.; Sing, K. S. W.; *Adsorption, Surface Area and Porosity*, Academic Press: New York, 1982.